POLITECNICO DI TORINO
Repository ISTITUZIONALE

A global–local approach for progressive damage analysis of fiber-reinforced composite laminates

*Original*
A global–local approach for progressive damage analysis of fiber-reinforced composite laminates / Nagaraj, M.H., Petrolo, M., Carrera, E.. - In: THIN-WALLED STRUCTURES. - ISSN 0263-8231. - ELETTRONICO. - 169:(2021). [10.1016/j.tws.2021.108343]

*Availability:*
This version is available at: 11583/2921294 since: 2021-09-06T09:06:07Z

*Publisher:*
Elsevier

*Published*
DOI:10.1016/j.tws.2021.108343

*Terms of use:*

This article is made available under terms and conditions as specified in the corresponding bibliographic description in the repository

*Publisher copyright*

(Article begins on next page)

16 October 2026

# A global-local approach for progressive damage analysis of fibre-reinforced composite laminates

M.H. Nagaraj, M. Petrolo, and E. Carrera

MUL$^2$ Group, Department of Mechanical and Aerospace Engineering, Politecnico di Torino,
Corso Duca degli Abruzzi 24, 10129 Torino, Italy

Submitted to Thin-Walled Structures

*Author for correspondence:*
M. Petrolo, Associate Professor
MUL$^2$ Group, Department of Mechanical and Aerospace Engineering,
Politecnico di Torino,
Corso Duca degli Abruzzi 24,
10129 Torino, Italy,
tel: +39 011 090 6845,
fax: +39 011 090 6899,
e-mail: marco.petrolo@polito.it

## *Abstract*

*The present work applies the global-local technique to the progressive damage analysis of fiber-reinforced composite laminates. A two-step global-local approach is developed as a combination of a low-fidelity linear global analysis and a high-fidelity local nonlinear analysis of specific regions within the structure, where damage is expected to occur. The local model is based on higher-order structural theories derived using the Carrera Unified Formulation, and specifically, Lagrange polynomials are used to model each ply through its thickness, leading to a layer-wise model. Composite damage is described using the CODAM2 material model, which is based on continuum damage mechanics. Initial assessments compare the relative performance of 3D-FE, 1D-CUF, and the proposed global-local approach via the free-edge stress analysis of a stiffened composite plate. The proposed technique is then used to predict the tensile strength of an open-hole specimen. The last assessment simulates damage progression within an over-height compact tension specimen using the global-local approach. The results demonstrate the accurate evaluation of 3D stress fields and composite laminates' mechanical response in the progressive damage regime. A multi-fold improvement in the computational cost is shown when compared to full-scale CUF analyses and indicates this technique's strong potential towards the computationally-efficient high-fidelity analysis of complex and large-scale composite structures.*



**Keywords**: global-local analysis, progressive damage analysis, CUF, CODAM2

# 1 Introduction

Fiber-reinforced composites are a popular choice as engineering materials due to their higher specific strength and stiffness than conventional metals. However, such materials tend to exhibit a very complex nonlinear response due to multiple failure modes' presence and interaction. Composite design based on a physical testing approach can be cumbersome due to the large design space associated with this class of materials. Therefore virtual testing methodologies offer an alternative approach to the design and analysis of composite structures.

The numerical analysis of composite structures requires accurate damage models to consider the influence of the various failure modes on the global structural response, and such material models tend to be computationally intensive. Furthermore, damage simulation often necessitates a high-fidelity - often 3D - numerical model of the structure, since nonlinear material models typically require accurate stress and strain inputs [1]. Combining these two issues results in the numerical modeling of progressive damage in composites structures being a challenging and computationally expensive task. Even with the availability of modern computing capabilities, composite damage simulations generally require analysis times ranging from hours to days on HPC systems [2, 3]. Such bottlenecks often force analysts to compromise between the accuracy and costs of the solution. This process introduces errors in the results and requires larger factors of safety, leading to conservative designs and an overall increase in the mass of the composite structure. The development of computationally-efficient and accurate virtual testing methods is therefore crucial to accelerate the adoption of composites within various engineering sectors and fully exploit the potential of such materials.

A popular approach to reducing computational costs without sacrificing the fidelity of the solution is the global-local technique. Conceptually, this method involves the low-fidelity modeling of the global structure, and only the critical regions of interest within the structure are modeled in high-fidelity. The local high-fidelity analysis is generally driven using information obtained from the global low-fidelity analysis. Global-local techniques were first developed in the past decades when computing power was extremely limited, and were successfully applied to both linear [4–8], and nonlinear problems [9, 10]. These techniques remain relevant in present times, even with modern computing capabilities, due to the computationally intensive nature of problems involving progressive damage. Global-local approaches have been used to investigate intra- and interlaminar damage in composite stiffened panels [11, 12]. A particular type of global-local analysis involves solid/shell coupling, which combines a 2D global model and a 3D model of the critical regions. The two models are generally connected using tie-constraints and are solved simultaneously within a single analysis. This approach has been used in the simulation of composite delamination and stiffener-skin debonding [13, 14]. Similar global-local approaches have been used in recent years to investigate progressive damage in composite laminates subjected to low-velocity impact, where tie-constraints are used to connect the global and local meshes [15–17].

The present work combines the global-local approach with higher-order structural theories derived using the Carrera Unified Formulation (CUF) [18]. In this approach, 2D expansion functions and 1D thickness functions are used to enhance the kinematics of 1D and 2D FE models, respectively, leading to solutions approaching

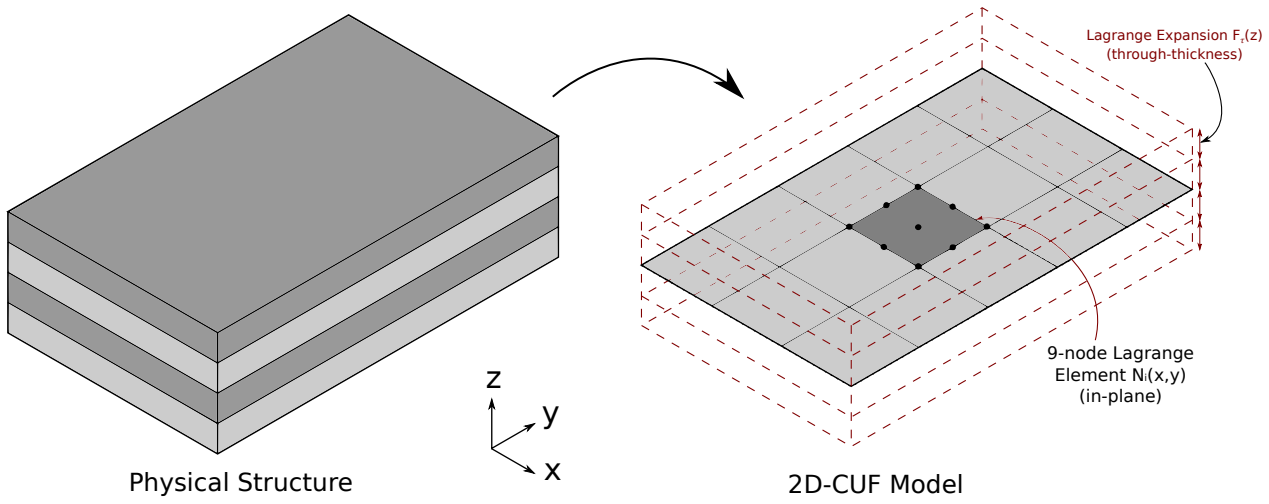


**Figure 1:** Layer-wise modeling of composite laminates in CUF.

that of 3D-FEA at significantly reduced computational costs [19]. In recent years, the efficiency and accuracy of CUF models have been demonstrated in various applications such as micromechanical and multiscale analysis [20, 21], contact modeling [22, 23], progressive damage and low-velocity impact analysis [24, 25], and the global-local interfacing of CUF theories with existing commercial software for linear and nonlinear analysis [26, 27]. The current work extends previous developments of global-local techniques in CUF, see Ref. [27], for the case of progressive damage in fiber-reinforced composites, using the continuum damage mechanics-based CODAM2 material model [24, 28, 29]. This paper is organized as follows: Section 2 provides an overview of CUF-based theories and their finite element (FE) formulation, while Section 3 describes the two-step global-local approach used in the current work. A series of numerical assessments are presented in Section 4 as verification and validation cases for the proposed approach. Section 5 summarises the conclusions of the present work.

## 2 Structural theories and FE formulation

The present work uses 2D-CUF theories to develop layer-wise models of multilayered structures and is briefly described in the following; see Ref. [24] for further details. The layer-wise CUF model consists of a combination of 2D FE and 1D Lagrange polynomials, as shown schematically in Fig. 1. This approach leads to the following description of the displacement field

$$\mathbf{u}(x,y,z) = F_\tau(z)\mathbf{u}_\tau(x,y), \tau = 1,2,\dots M \tag{1}$$

where $\mathbf{u}_\tau(x,y)$ is the generalized in-plane displacement, and $F_\tau(z)$ represents a 1D expansion function, with $M$ terms, that describes the kinetic interpolation through the thickness of each layer within the laminate. $F_\tau(z)$ and $M$ can be selected by the user and determines the model's structural theory. As seen in Fig. 1, the present work adopts 1D Lagrange polynomials as $F_\tau(z)$, and this type of expansion function is referred to as the

Lagrange-Expansion (LE) class in CUF. The LE modeling approach leads to a layer-wise 2D model which can evaluate 3D field variables and consists of solely translational degrees of freedom (DOF). A detailed overview of 2D CUF models based on the LE class is found in [18].

## Finite element formulation

The 3D stress and strain fields are denoted by

$$\begin{aligned} \boldsymbol{\sigma} &= \{\sigma_{xx}, \sigma_{yy}, \sigma_{zz}, \sigma_{xy}, \sigma_{xz}, \sigma_{yz}\} \\ \boldsymbol{\varepsilon} &= \{\varepsilon_{xx}, \varepsilon_{yy}, \varepsilon_{zz}, \varepsilon_{xy}, \varepsilon_{xz}, \varepsilon_{yz}\} \end{aligned} \tag{2}$$

The displacement-strain relation, assuming geometrical linearity, is written as

$$\boldsymbol{\varepsilon} = \mathbf{D}\mathbf{u} \tag{3}$$

where $\mathbf{u}$ is the displacement vector. The linear differential operator $\mathbf{D}$ is defined as

$$\mathbf{D} = \begin{bmatrix} \frac{\partial}{\partial x} & 0 & 0 \\ 0 & \frac{\partial}{\partial y} & 0 \\ 0 & 0 & \frac{\partial}{\partial z} \\ \frac{\partial}{\partial y} & \frac{\partial}{\partial x} & 0 \\ \frac{\partial}{\partial z} & 0 & \frac{\partial}{\partial x} \\ 0 & \frac{\partial}{\partial z} & \frac{\partial}{\partial y} \end{bmatrix}$$

Considering material nonlinearities, the constitutive relation is given by

$$\boldsymbol{\sigma} = \mathbf{C}^{sec}\boldsymbol{\varepsilon} \tag{4}$$

where $\mathbf{C}^{sec}$ is the secant stiffness matrix, and depends on the material model used in the analysis. The in-plane geometry is discretized using 2D FE, such as 9-node (Q9) quadrilateral elements with shape functions $N_i(x, y)$, and in combination with 1D LE functions through the thickness, leads to the following description of the 3D displacement field

$$\mathbf{u}(x, y, z) = N_i(x, y)F_\tau(z)\mathbf{u}_{\tau i} \tag{5}$$

The semi-discrete balance of momentum is

$$\mathbf{M}\ddot{\mathbf{u}} = \mathbf{F}_{ext} - \mathbf{F}_{int} \tag{6}$$

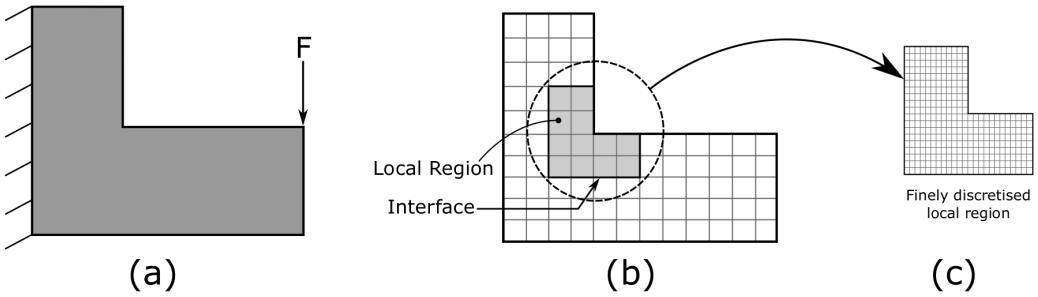


**Figure 2:** Schematic representation of the generalised two-step sequential global-local approach. (a) The physical structure, (b) coarsely discretized (low-fidelity) global model, and (c) finely discretized (high-fidelity) local model of the critical region.

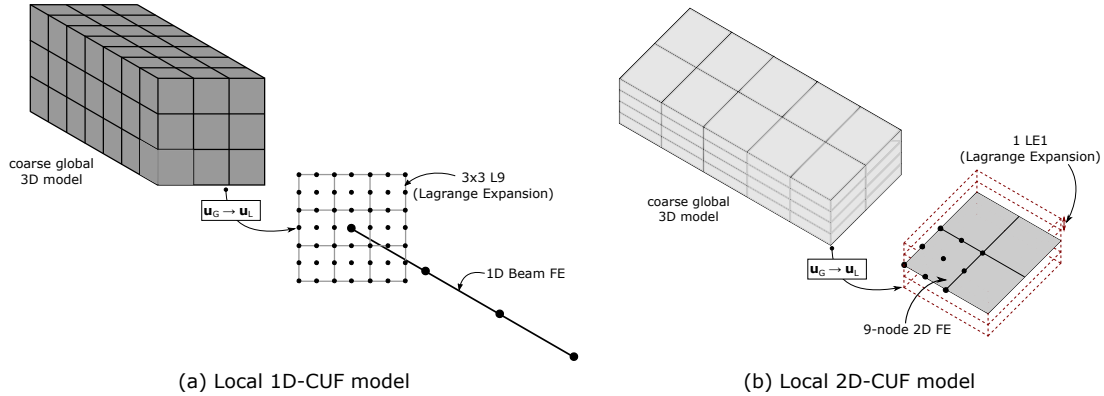


**Figure 3:** Global-local approach using higher-order CUF theories to model the local region.

where $\mathbf{M}$ is the mass matrix and $\ddot{\mathbf{u}}$ is the acceleration vector. The external and internal force vectors are denoted by $\mathbf{F}_{ext}$ and $\mathbf{F}_{int}$, respectively. The nonlinear system of equations is solved using explicit time integration, and a detailed description of explicit nonlinear analysis using CUF theories is available in [24].

# 3 Global-local analysis

The two-step sequential global-local scheme is considered in the present work and extends previous developments in nonlinear global-local analysis [27]. This approach, in general, consists of two separate analyses - (1) a low-fidelity model of the global structure and (2) a high-fidelity model of the local region under investigation. The solution obtained from the global analysis, usually in the form of displacement fields, is applied to drive the local analysis. A schematic representation of the generalized two-step sequential global-local approach is shown in Fig. 2, where the local model's fidelity is improved by using a finer discretization. The current work uses this technique to interface the commercial FE code ABAQUS with the academic MUL2 code, a stand-alone numerical platform based on CUF structural theories and written in Fortran. The low-fidelity global model is thus developed using a coarsely discretized 3D-FE model in ABAQUS, while the critical region of interest is modeled in high fidelity using higher-order CUF structural theories. Both 1D- and 2D-CUF structural theories can be utilized to develop the high-fidelity local models, as seen in Fig. 3. The nodal displacements obtained

**Table 1:** Elastic and strength properties of the IM7/8552 CFRP material system. [30]

| $E_1$ [GPa] | $E_2$ [GPa] | $E_3$ [GPa] | $G_{12}$ [GPa] | $G_{13}$ [GPa] | $G_{23}$ [GPa] | $\nu_{12}$ | $\nu_{13}$ | $\nu_{23}$ |
|---|---|---|---|---|---|---|---|---|
| 165.0 | 9.0 | 9.0 | 5.6 | 5.6 | 2.8 | 0.34 | 0.34 | 0.5 |
| | | $X_T$ [MPa] | $Y_T$ [MPa] | $S_L$ [MPa] | $G_1^f$ $[kJ/m^2]$ [31] | $G_2^f$ $[kJ/m^2]$ [32] | | |
| | | 2560.0 | 73.0 | 90.0 | 120.0 | 2.6 | | |

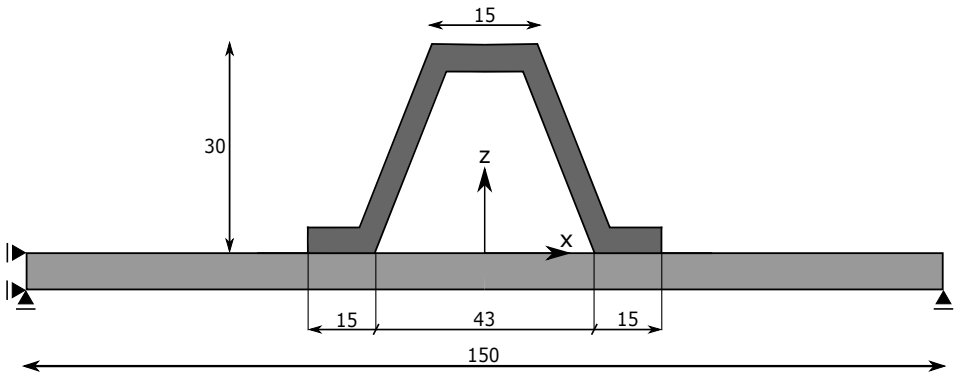


**Figure 4:** Schematic representation of the stiffened composite panel cross-section. All dimensions in mm.

from the global linear-elastic 3D-FE analysis are applied as displacement-based boundary conditions in the local CUF models. Compatibility between the global and local meshes is not required since the global nodal displacements are interpolated before applying them to the local models. This technique applies to nonlinear analysis when the nonlinear region remains localized and can thus be included within the local domain (see Ref. [27] for the case of localized plasticity). The present work investigates localized damage in fiber-reinforced composites subjected to tensile loads via the global-local approach. The CODAM2 material model, previously implemented in the CUF framework [24], is used to simulate composite damage in the local CUF analysis.

# 4 Numerical Examples

This section presents a series of numerical cases to verify and validate the proposed global-local approach. The focus is on the high-fidelity stress and progressive damage analysis of laminated composite structures. The material system considered in each assessment is the IM7/8552 carbon fiber-reinforced polymer (CFRP), with a nominal ply thickness of 0.125 mm. The elastic and strength properties of the composite material are listed in Table 1.

## 4.1 Free-edge stress analysis of stiffened composite panel

The current example investigates the proposed global-local approach's performance in accurately evaluating interlaminar stresses and failure indexes in composite laminates based on linear analysis. The aim is to verify the results as the proper detection of stresses and failure indexes plays a crucial role in the progressive failure.

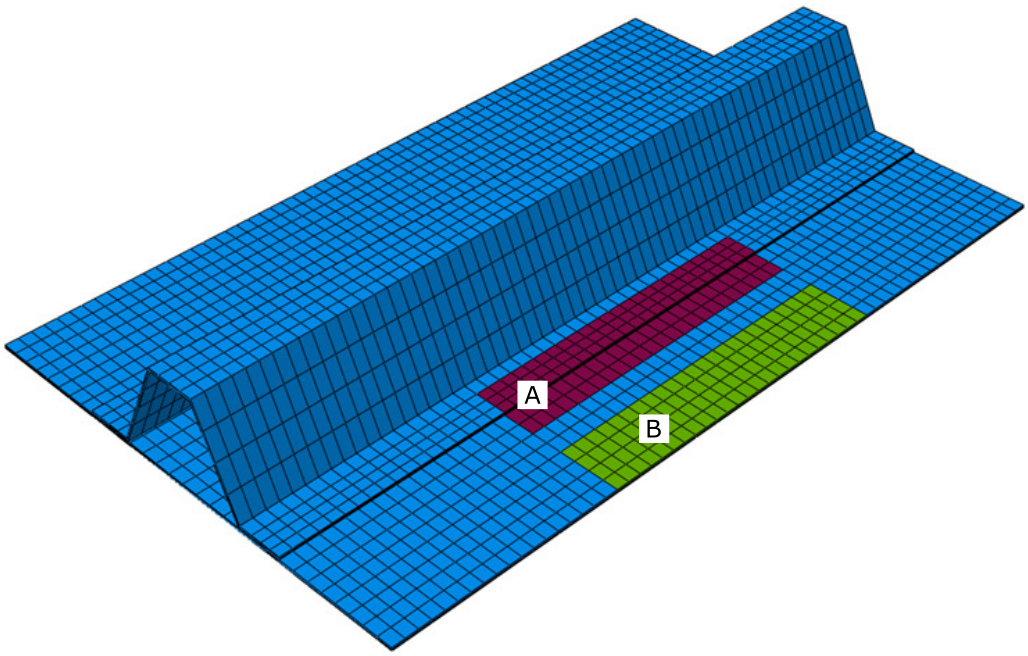


**Figure 5:** Low-fidelity global 3D-FE model of the stiffened composite panel, with local regions for free-edge stress evaluation highlighted.

The structure consists of a composite plate stiffened with a composite trapezoidal stringer, as shown in Fig. 4, and spans 240 mm along the $y$-axis. The panel is a 1 mm thick $[45/90/-45/0]_s$ quasi-isotropic laminate, and the trapezoidal stringer is a 0.875 mm thick $[-45/0/45/0/45/0/-45]$ laminate. The structural geometry was first proposed by Bisagni et al. [33]. The structure is subjected to a tensile load, and the objective of the numerical assessment is to evaluate the stresses at the free-edge of the stringer and the panel. Reference solutions based on high-fidelity 3D-FE and 1D-CUF models of the full structure were presented in [19].

A low-fidelity 3D-FE model of the global structure is first considered, and two critical regions are selected for the high-fidelity local CUF analysis, as shown in Fig. 5. In a subsequent step, a high-fidelity local analysis is performed using 1D-CUF models of the required local domains. The size of the local region was chosen based on the stress fields obtained from [19]. In the next sections, convergence analyses regarding the local region size are presented.

The interlaminar stress components at the free-edge of the stringer (Region A) and panel (Region B) are plotted in Fig. 6 and Fig. 7, respectively. Failure indices to indicate the initiation of matrix tension damage - 3D Hashin failure theory [34] - and delamination - mixed-mode quadratic criterion [35] - are also computed at the free-edge of the stringer, Fig. 8, and at the panel free-edge, Fig. 9. In each case, reference high-fidelity 3D-FE and 1D-CUF results and that of the low-fidelity global 3D-FE used to inform the local analysis have been overlaid for comparison. Details of the various numerical models are listed in Table 2. The results suggest that

1. The interlaminar stress fields predicted by the local CUF analysis are in good agreement with those obtained by the high-fidelity analysis of the global structure, as seen in Fig. 6 and Fig. 7, thus verifying

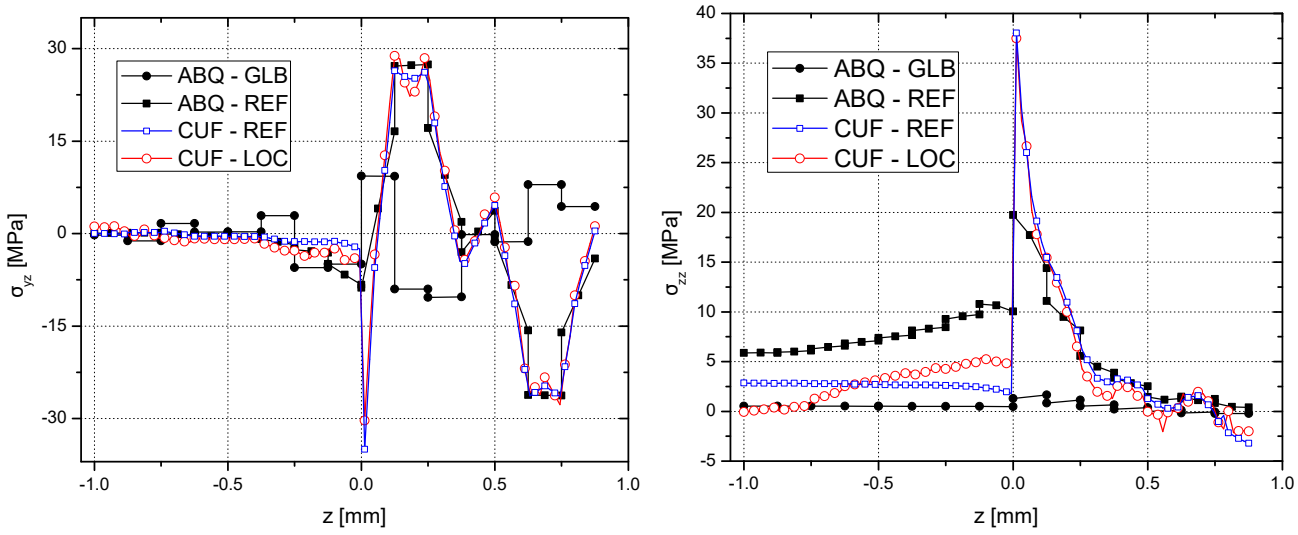


**(a)** $\sigma_{yz}$ **(b)** $\sigma_{zz}$

**Figure 6:** Free-edge interlaminar stresses through the thickness of the composite stringer. Reference numerical results from [19].

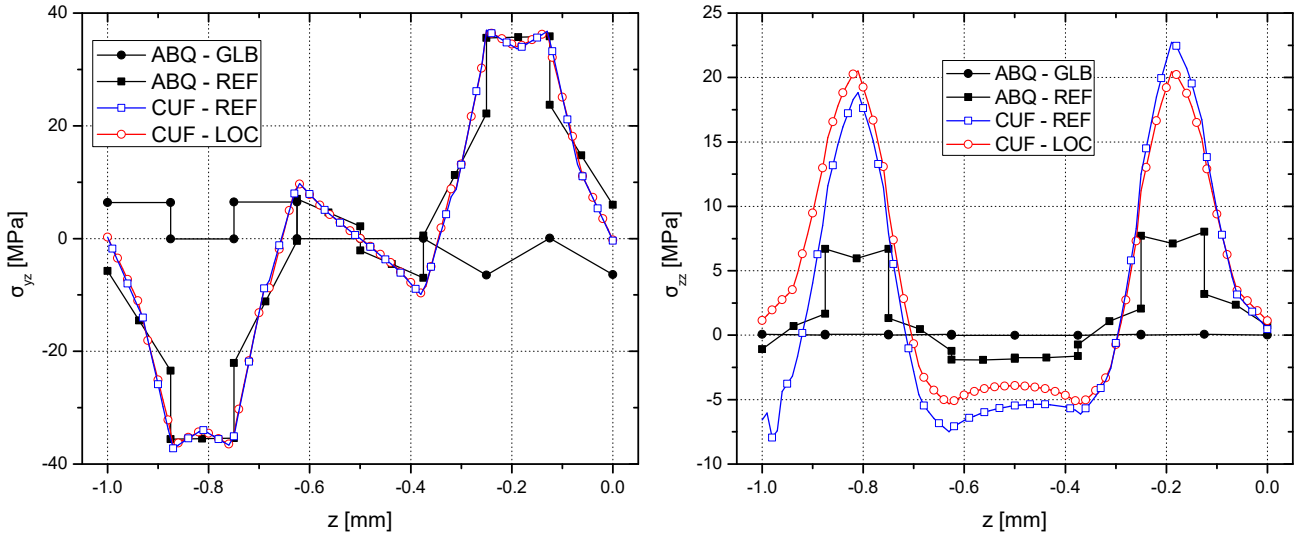


**(a)** $\sigma_{yz}$ **(b)** $\sigma_{zz}$

**Figure 7:** Free-edge interlaminar stresses through the thickness of the composite panel. Reference numerical results from [19].

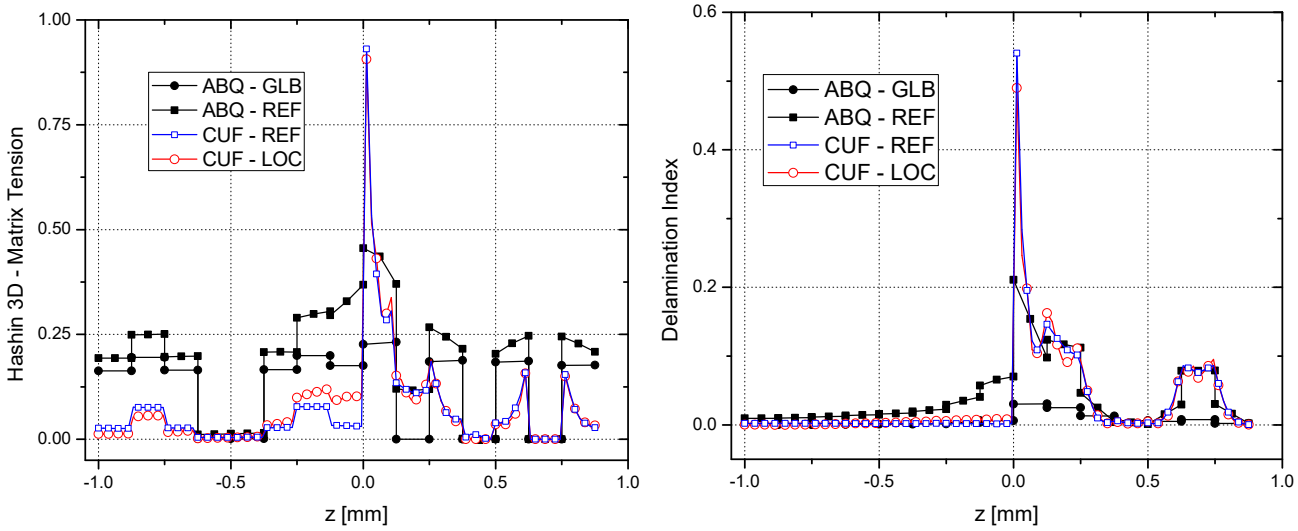


**(a)** Hashin 3D - Matrix tension **(b)** Delamination index

**Figure 8:** Failure indices evaluated at the free-edge of the composite stringer. Reference numerical results from [19].

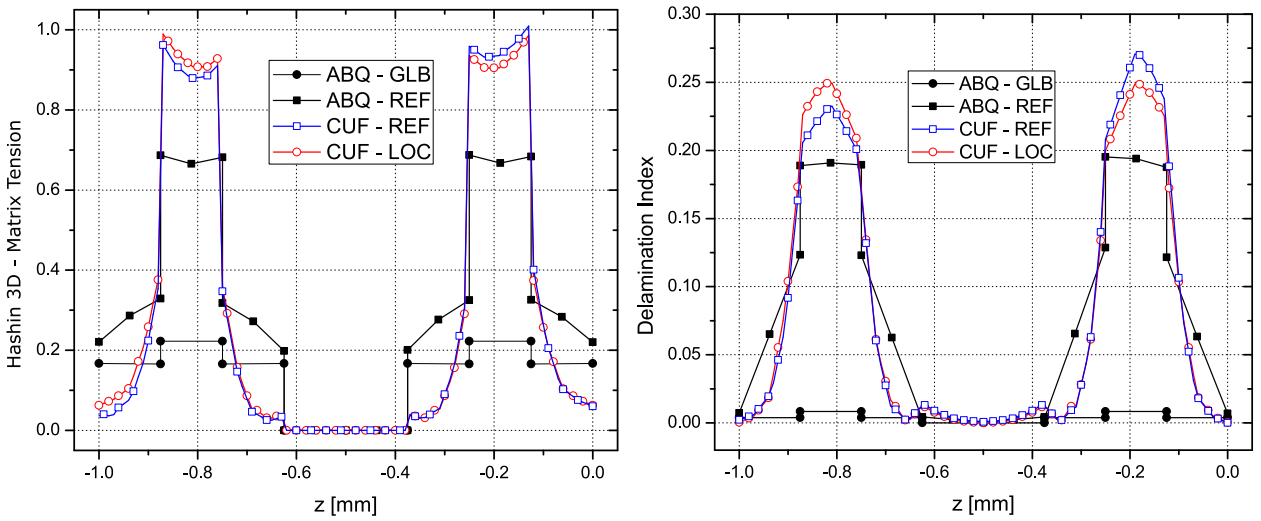


**(a)** Hashin 3D - Matrix tension **(b)** Delamination index

**Figure 9:** Failure indices evaluated at the free-edge of the composite panel. Reference numerical results from [19].

**Table 2:** Details of the various numerical approaches used for the free-edge analysis of the stiffened composite panel.

| Model | Element Type | DOF | Time (s) |
|---|---|---|---|
| | **Reference global high-fidelity models** [19] | | |
| ABQ-3D | 1,411,200 C3D8 (2 elem/ply) | 4,560,150 | 3,764 |
| CUF-LW | 710 L9, 10 B4 (2 L9/ply) | 277,326 | 478 |
| | **Low-fidelity global analysis** | | |
| ABQ-3D | 22,800 C3D8 (1 elem/ply) | 81,801 | 8 |
| | **High-fidelity local analysis** | | |
| CUF-LW (Region A) | 112L9, 6 B4 (2 L9/ply) | 28,215 | 25 |
| CUF-LW (Region B) | 92L9, 6 B4 (2 L9/ply) | 24,909 | 22 |

the proposed global-local approach.

2. The global (low-fidelity) 3D-FE results significantly underestimate the interlaminar stress field and consequently the failure indices, as seen in Fig. 8 and Fig. 9. However, the global displacement field is sufficient to drive the local CUF analysis and leading to accurate stress evaluations by the local model.

3. The previous observation also highlights the importance of the accurate evaluation of stress fields by the structural models. Insufficiently refined models underestimate the stress fields, leading to lower magnitudes of failure indices used as failure initiation criteria, and may result in delayed damage initiation and progression.

4. The global, reference 3D-FE solution, while more accurate than that obtained by the low-fidelity global 3D model, still has considerable variations compared to the global CUF results as the latter have a more refined kinematics through-the-thickness. The further refinement of the 3D mesh could reduce the differences but increase the computational costs; see Ref. [19] for a detailed discussion.

5. The proposed global-local approach is approximately $15x$ faster than the reference global CUF analysis and about $114x$ faster than the corresponding refined global 3D analysis. This demonstrates significant improvements in the computational efficiency of this technique compared to global high-fidelity analyses.

## 4.2 Tensile strength prediction of open-hole specimen

The present numerical assessment constitutes a further verification step towards using the proposed global-local approach in composite damage analysis. The structure is an open-hole tension (OHT) specimen, based on the experimental works of Green et al. [36]. The aim is to predict the specimen's tensile strength. A schematic view of the global structure is shown in Fig. 10. The lamination is $[45/90/-45/0]_{8s}$ with a total thickness of 8 mm, see Table 1. The specimen fails under brittle fracture localized near the central hole [36] and hence is a suitable validation case for the proposed technique.

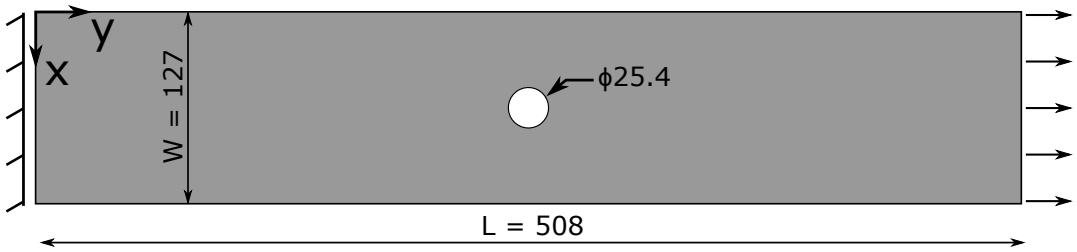


**Figure 10:** Schematic representation of the $[45/90/-45/0]_{8s}$ IM7/8552 CFRP open-hole tension specimen. All dimensions in mm.

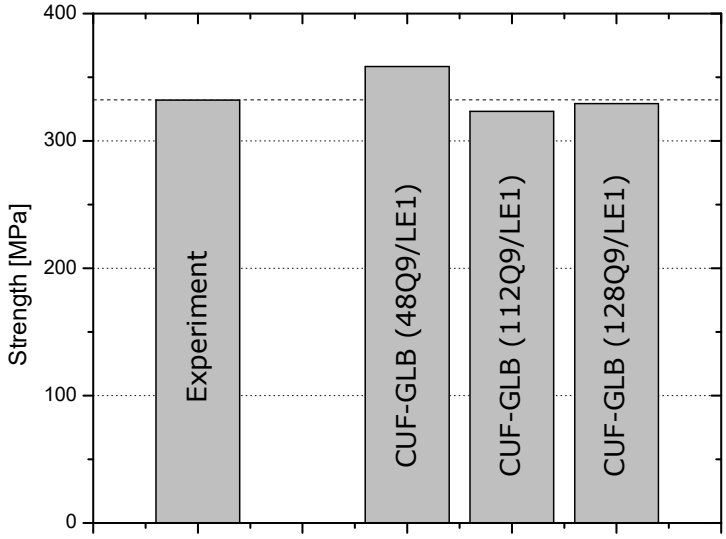


**Figure 11:** Tensile strength predicted by the various CUF models of the global OHT specimen. Experimental results obtained from [36].

A series of assessments are first performed over the global OHT structure, using layer-wise 2D-CUF models of increasing in-plane refinement and provide numerical reference results. A linear Lagrange expansion function (LE1) was used to model individual plies in the thickness direction and is sufficient considering the problem's in-plane nature. The tensile strengths predicted by the various global CUF models are plotted in Fig. 11. Then, the global-local approach is applied to the problem, with the central region containing the through-hole being retained for the high-fidelity local analysis, as shown in Fig. 12. A series of CUF models, with progressive in-plane refinement, are used to analyze the local region containing the hole, and the predicted tensile strengths are plotted in Fig. 13. Details of the numerical models are summarised in Table 3. The following observations are made:

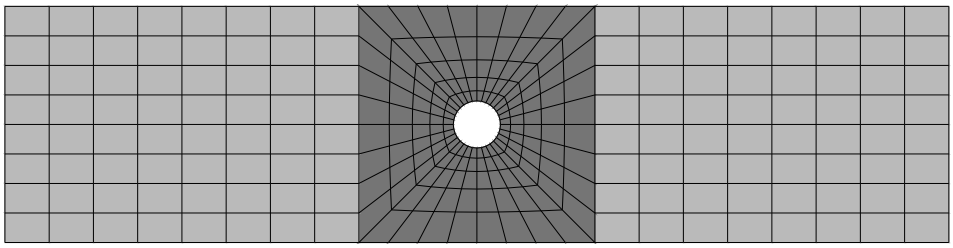

**Figure 12:** Low-fidelity global 3D-FE model of the OHT specimen with the domain for local analysis highlighted.

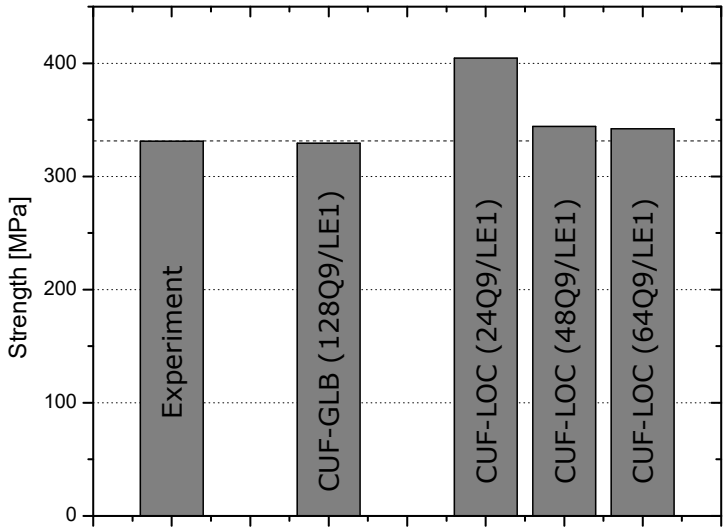


**Figure 13:** Tensile strength predicted by the various local CUF models. Experimental results obtained from [36].

**Table 3:** Model information for the tensile strength prediction of $[45/90/-45/0]_{4s}$ quasi-isotropic OHT specimen.

| Model | Discretization of the open-hole specimen | DOF | Analysis Time* [hh:mm:ss] |
|---|---|---|---|
| | **Reference 2D-CUF (global structure)** | | |
| CUF GLB - 48Q9/LE1 | 48 Q9 elements in-plane (1 LE1/ply) | 45,240 | 1:00:47 |
| CUF GLB - 112Q9/LE1 | 112 Q9 elements in-plane (1 LE1/ply) | 98,280 | 2:50:19 |
| CUF GLB - 128Q9/LE1 | 128 Q9 elements in-plane (1 LE1/ply) | 110,760 | 3:16:03 |
| | **Low-fidelity 3D-FE (global structure)** | | |
| ABQ-3D | 18,432 C3D8R (1 elem/ply) | 65,520 | 0:01:29 |
| | **High-fidelity 2D-CUF (local region)** | | |
| CUF LOC - 24Q9/LE1 | 24 Q9 elements in-plane (1 LE1/ply) | 21,840 | 0:26:25 |
| CUF LOC - 48Q9/LE1 | 48 Q9 elements in-plane (1 LE1/ply) | 43,680 | 0:59:00 |
| CUF LOC - 64Q9/LE1 | 64 Q9 elements in-plane (1 LE1/ply) | 56,160 | 1:27:02 |

* The reported run-times are based on analyses performed on a desktop computer using 4 cores.

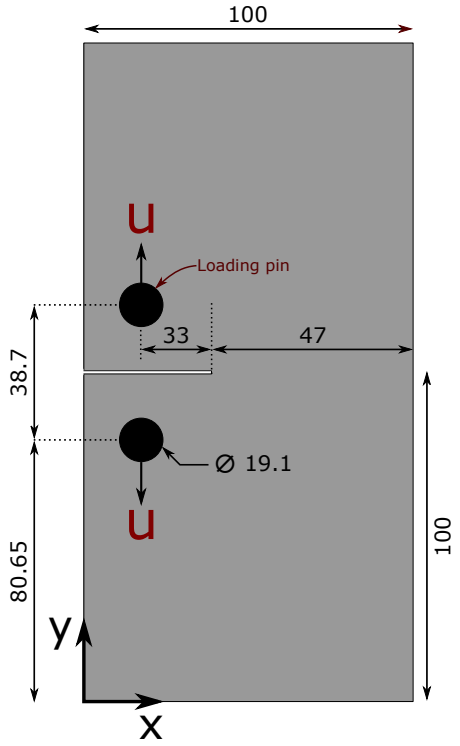


**Figure 14:** Schematic representation of the $[90/45/0/-45]_{4s}$ IM7/8552 CFRP over-height compact tension specimen. All dimensions in mm.

1. The CUF models of the global OHT specimen can successfully predict tensile strength values in very close agreement with experimental data (error<1%).

2. The application of the global-local approach leads to tensile strength predictions, which are in reasonable agreement with experimental data (error∼3%). The investigated OHT specimen consists of 64 plies, and the global-local approach is a convenient way of modeling such thick laminates, in high-fidelity, at reasonable computational overheads.

3. Comparing the coarsest global and local CUF models which provide a reasonably accurate tensile strength prediction, i.e., the CUF-GLB (112Q9/LE1, error = 2.6%) and CUF-LOC (48Q9/LE1, error = 3.7%) models, respectively, it is seen that the use of global-local techniques leads to an approximately $2.8x$ improvement in the overall analysis time.

## 4.3 Progressive damage analysis of over-height compact tension specimen

This numerical example focuses on the progressive damage analysis of the over-height compact tension (OCT) specimen, investigated previously using full-scale 2D-CUF models in [24]. The OCT specimen is schematically shown in Fig. 14, and is based on a 4 mm thick $[90/45/0/-45]_{4s}$ IM7/8552 CFRP quasi-isotropic composite laminate, see Table 1.

The present assessment uses the global-local approach to evaluate progressive damage in the OCT specimen. The influence of the local region's choice is first investigated by selecting three increasingly larger regions labeled

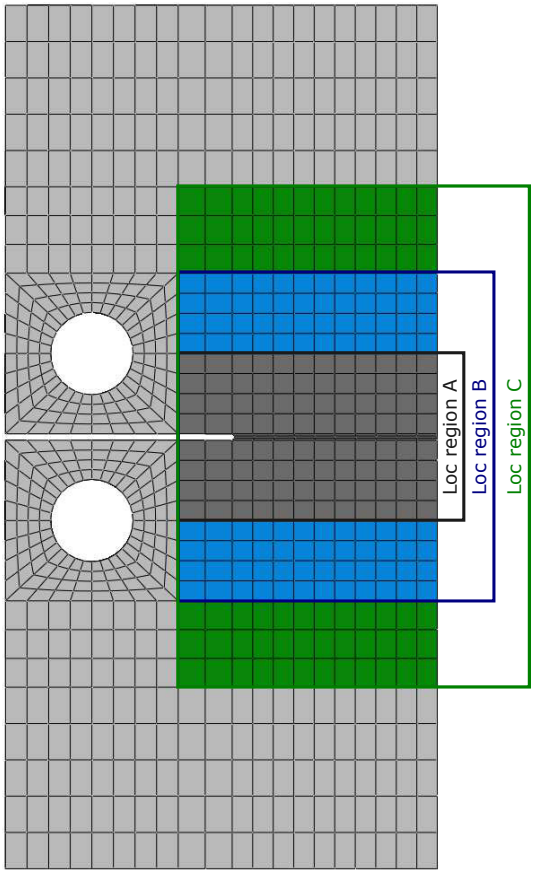


**Figure 15:** Low-fidelity 3D-FE model of the global OCT specimen with the local regions highlighted.

A, B, and C, respectively. Figure 15 shows the global low-fidelity 3D-FE model with the three regions considered for the high-fidelity local CUF analysis highlighted. Two 2D-CUF models have been developed for each local region, with a progressive refinement of the in-plane discretization, and the refined model is discretized using the same mesh density as the reference global CUF analysis. In this case, all the CUF models are built with a single linear Lagrange polynomial function (LE1) to represent each ply's thickness.

The force-displacement response obtained from the local CUF models has been plotted in Fig. 16, with experimental data from [37] and reference global CUF results from [24] overlaid for comparison. Contour plots of the matrix and fiber damage in the 90° and 0° plies, respectively, are shown in Fig. 17, for a POD of 1.5 mm. The damage state predicted by the reference global CUF model is also included for comparison. The last assessment studies the influence of the Lagrange polynomial (LE) order used to model the individual ply thickness and based on the results seen in Fig. 16, the global-local analysis is performed using the local region B. The force-displacement response obtained by the local CUF models is plotted in Fig. 18, with reference to global CUF results for comparison. Details of the various numerical models are summarised in Table 4. The following comments are made:

1. The influence of the domain considered for the local analysis can be seen in the force-displacement plots of Fig. 16. Selecting a very small local domain (region A) results in the global-local interface being very

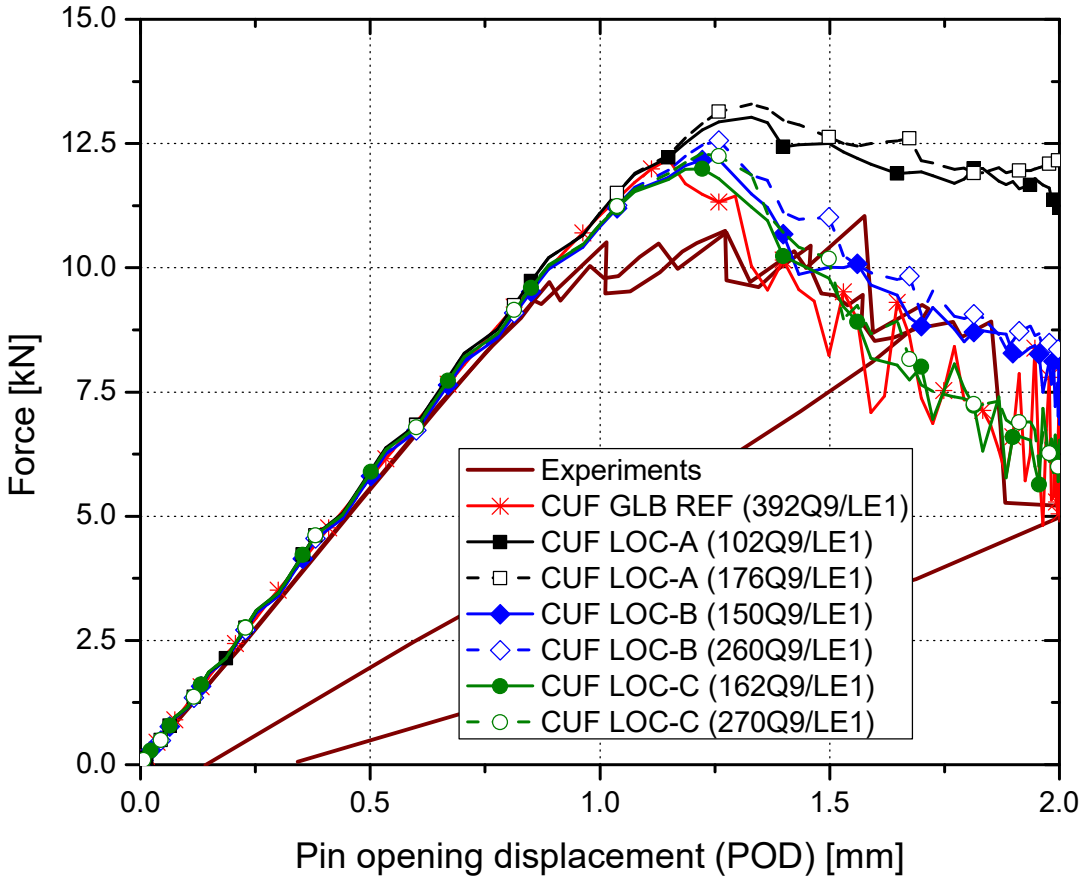


**Figure 16:** POD-force curves of the $[90/45/0/-45]_{4s}$ IM7/8552 CFRP over-height compact tension specimen. Experimental data is obtained from [37] and reference CUF results are from [24].

**Table 4:** Model information for the progressive damage analysis of the $[90/45/0/-45]_{4s}$ IM7/8552 CFRP over-height compact tension specimen.

| Model | Discretization of the OCT specimen | DOF | Analysis Time* [hh:mm:ss] |
|---|---|---|---|
| | **Reference 2D-CUF (global structure)** | | |
| CUF 392Q9/LE1 | 392 Q9 elements in-plane (1 LE1/ply) | 164,925 | 11:17:42 |
| | **Low-fidelity 3D-FE (global structure)** | | |
| ABQ-3D | 25,536 C3D8R (1 elem/ply) | 88,506 | 00:02:26 |
| | **High-fidelity 2D-CUF (local region)** | | |
| CUF LOC-A (102Q9/LE1) | 102 Q9 elements in-plane (1 LE1/ply) | 45,045 | 02:12:00 |
| CUF LOC-A (176Q9/LE1) | 176 Q9 elements in-plane (1 LE1/ply) | 75,537 | 03:37:38 |
| CUF LOC-B (150Q9/LE1) | 150 Q9 elements in-plane (1 LE1/ply) | 64,845 | 02:55:01 |
| CUF LOC-B (260Q9/LE1) | 260 Q9 elements in-plane (1 LE1/ply) | 109,989 | 06:05:14 |
| CUF LOC-C (162Q9/LE1) | 162 Q9 elements in-plane (1 LE1/ply) | 69,597 | 03:23:08 |
| CUF LOC-C (270Q9/LE1) | 270 Q9 elements in-plane (1 LE1/ply) | 113,949 | 06:36:29 |
| CUF LOC-B (150Q9/LE2) | 150 Q9 elements in-plane (1 LE2/ply) | 127,725 | 06:52:14 |
| CUF LOC-B (150Q9/LE3) | 150 Q9 elements in-plane (1 LE3/ply) | 190,605 | 16:18:02 |

* The reported run-times are based on analyses performed on a desktop computer using 4 cores.

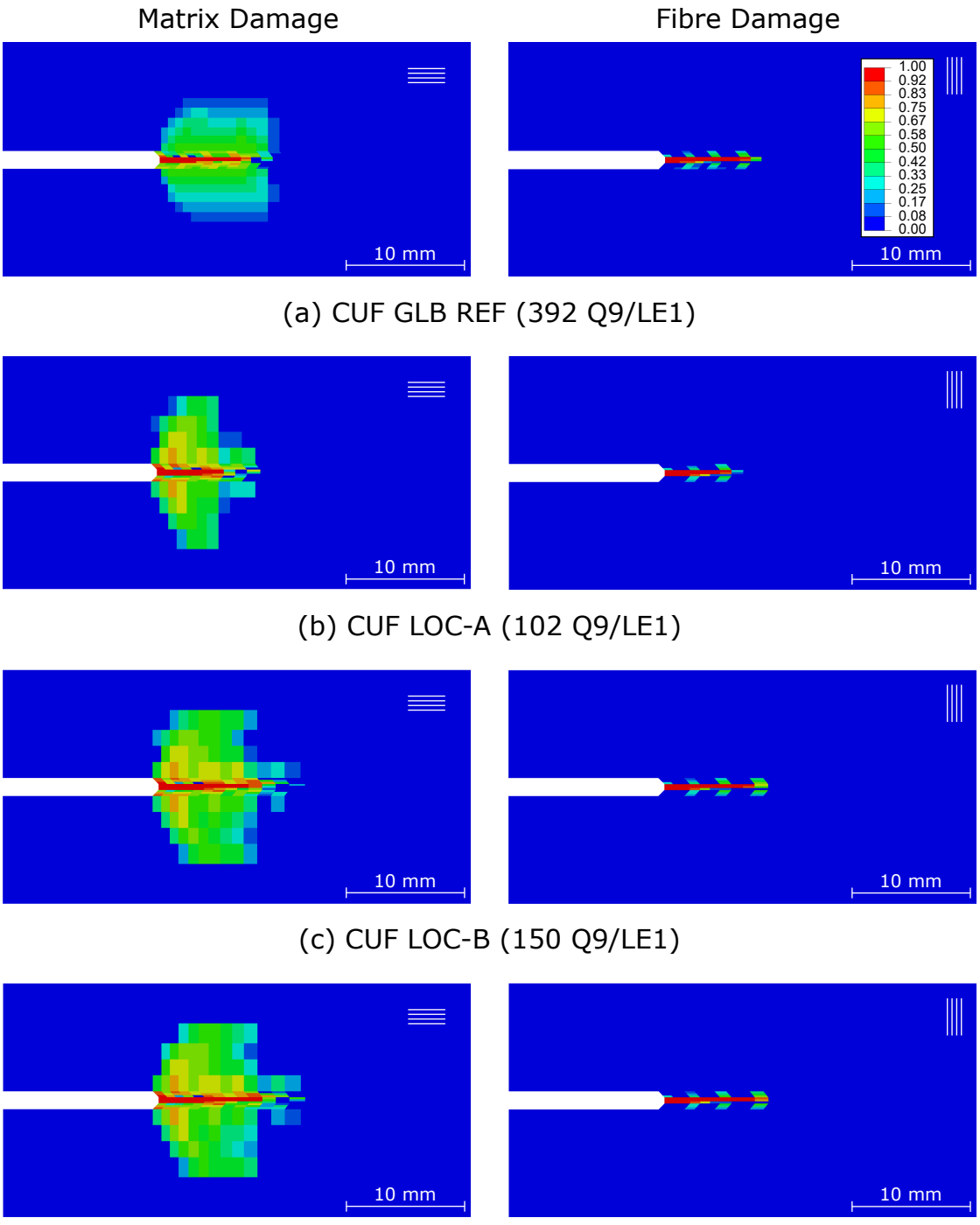


**Figure 17:** Distribution of matrix damage in the 90° ply (left) and fibre damage in the 0° ply (right) near the notch of the $[90/45/0/-45]_{4s}$ IM7/8552 CFRP OCT specimen predicted using the global-local approach. Reference global CUF solutions obtained from [24].

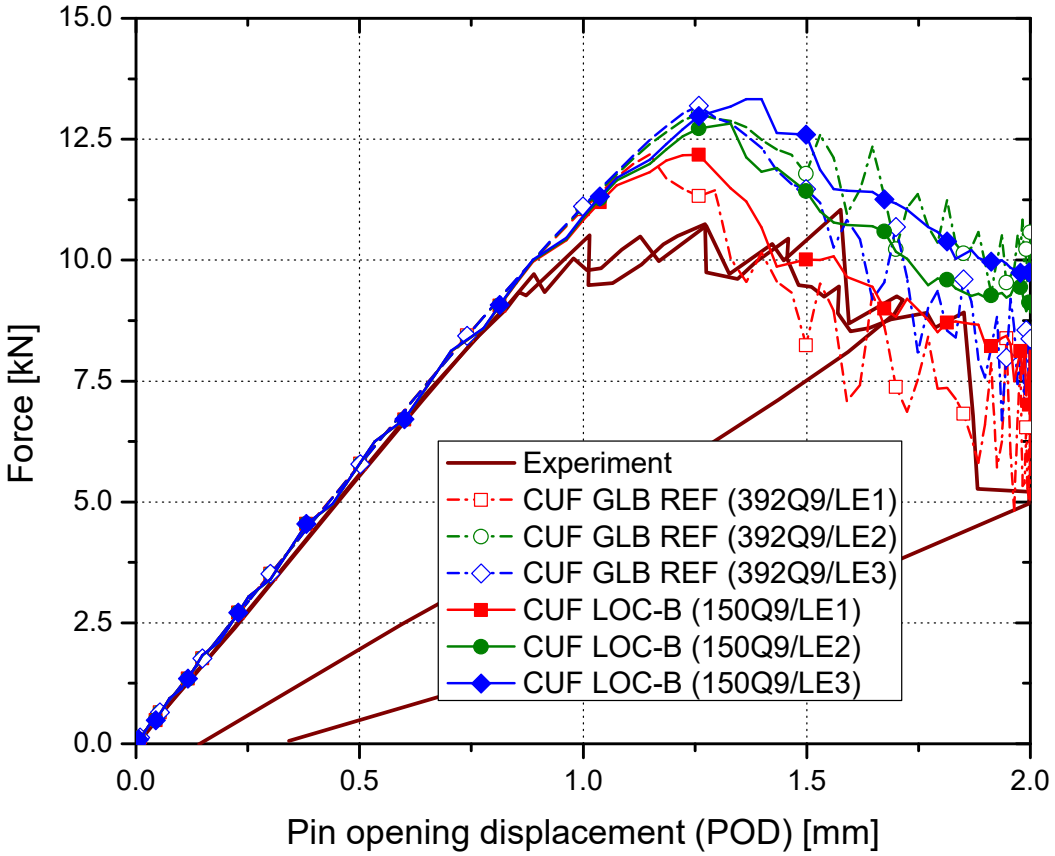


**Figure 18:** Influence of the thickness expansion function (LE) order on the POD-force curves of the $[90/45/0/-45]_{4s}$ IM7/8552 CFRP over-height compact tension specimen. Experimental data is obtained from [37] and reference CUF results are from [24].

close to the fracture process zone. The application of boundary conditions at this interface introduces a constraining effect that strongly influences the damage initiation and progression, leading to a delayed peak-point and a significant difference in the softening curve. Increasing the local domain size (regions B and C) shifts the interface to be sufficiently far-field, resulting in a better correlation between the predictions of the local and global CUF analyses.

2. Furthermore, the proximity of the interface to the fracture process zone and the resulting constraining effect leads to an inhibition of damage growth. This is seen in Fig. 17, as the local domain A leads to a smaller damaged area when compared to the reference global CUF predictions. Larger local domains (regions B and C), on the other hand, predict a damaged state which is in better agreement with the reference global CUF analysis.

3. The constraining effects of boundary conditions applied at the interface are also seen in the post-peak softening curve of the force-displacement response plotted in Fig. 16. The proximity of the interface in local region A leads to a large constraining effect and attenuates the oscillations. This causes the softening branch of the curve to be very smooth, even without numerical damping approaches. The use of progressively larger local domains reduces this constraining effect and consequently increases the oscillations in the post-peak response, as seen in Fig. 16 the case of regions B and C. The global analysis, which can be considered a limit case, results in the highest oscillatory response.

4. The use of progressively larger local domains serves as an 'area convergence' study, and the results obtained from the local CUF analysis of regions B and C are in relatively good agreement with each other and the global CUF solution. The local domain B can thus be considered to be sufficient for the local CUF analysis.

5. Two discretizations were used to model each local region, with the more refined model having the same mesh density as the reference global CUF model. From the force-displacement response (Fig. 16), it is seen that both discretizations effectively predict the same response, indicating convergence of the mesh. This suggests that the original global CUF model (see Ref. [24]) was more refined than required and was due to the need to model the entire global structure (including circular regions for the loading pins). The use of global-local techniques avoids the necessity of modeling such aspects of the global structure, and the computational effort can be focused on the critical regions under investigation, such as that in front of the notch.

6. The influence of the ply thickness expansion function (LE) is seen in Fig. 18. It is seen that the local CUF models with a particular expansion function (LE1, LE2, and LE3) are in good general agreement with the corresponding global CUF solutions. Higher-order theories tend to exhibit a more considerable amount of numerical oscillations, as seen in the global CUF models, and this is mostly attenuated by the

constraining effect present in the global-local approach seen in the local CUF models. Furthermore, a linear expansion function (LE1) is recommended in the current case due to the highly in-plane nature of the problem and is consistent with previous investigations (see Ref. [24]).

7. As detailed in [24], the numerical models do not consider delamination, which may account for the difference in peak load when compared to experimental data.

8. From Table 4, it is seen that the local CUF analysis of region B (150 Q9/LE1) leads to an approximately $3.8x$ speed-up of the analysis time when compared to the reference full-scale CUF analysis (392Q9/LE1). This demonstrates the significant computational efficiency that can be achieved, besides the intrinsic efficiencies of CUF models, via the proposed global-local approach.

# 5 Conclusion

The present work applies the two-step global-local approach towards the progressive damage analysis of fiber-reinforced composite laminates. A low-fidelity linear-elastic 3D-FE analysis is first performed, and the global displacements are applied as boundary conditions to a subsequent high-fidelity local analysis of the critical region where damage is expected to occur. The local models are developed using higher-order layer-wise 2D theories derived using the Carrera Unified Formulation, and progressive damage is described using the CODAM2 material model. The first numerical example assesses the free-edge stresses of a stiffened composite panel using the global-local approach and compares the proposed technique's performance with full-scale CUF and 3D-FE models. Next, the tensile strength of a composite laminate with a central hole is evaluated using the proposed approach. The predicted strengths are found to be in good agreement with experimental and reference global CUF results, thus providing initial validation of the global-local technique. Finally, this approach is applied to the progressive damage analysis of the over-height compact tension specimen. The influence of the local domain size and the distance from the global-local interface to the fracture process zone is investigated. It is shown that the proximity of the interface to the nonlinear zone has a constraining effect, leading to delayed damage initiation and progression, significantly affecting the solution quality. The presented numerical results demonstrate the capability of the proposed global-local approach in analyzing problems involving progressive damage in composite laminates and achieve a multi-fold improvement in computational time compared to full-scale CUF analysis of the global structure. This approach, combined with the capabilities of higher-order CUF models, can lead to significant savings in computational effort when dealing with the nonlinear structural analysis of complex composite structures. Future works aim to extend the developments to problems involving the impact in composite laminates.

## Acknowledgements

This research work has been carried out within the project ICONIC (Improving the Crashworthiness of Composite Transportation Structures), funded by the European Union Horizon 2020 Research and Innovation program under the Marie Skłodowska-Curie Grant agreement No. 721256.

## References

[1] YS Reddy and JN Reddy. Three-dimensional finite element progressive failure analysis of composite laminates under axial extension. *Journal of Composites, Technology and Research*, 15(2):73–87, 1993.

[2] EV González, P Maimí, PP Camanho, A Turon, and JA Mayugo. Simulation of drop-weight impact and compression after impact tests on composite laminates. *Composite Structures*, 94(11):3364–3378, 2012.

[3] G Perillo, NP Vedivik, and AT Echtermeyer. Damage development in stitch bonded gfrp composite plates under low velocity impact: Experimental and numerical results. *Journal of Composite Materials*, 49(5):601–615, 2015.

[4] JB Ransom and NF Knight Jr. Global/local stress analysis of composite panels. *Computers & structures*, 37(4):375–395, 1990.

[5] KM Mao and CT Sun. A refined global-local finite element analysis method. *International journal for numerical methods in engineering*, 32(1):29–43, 1991.

[6] JD Whitcomb. Iterative global/local finite element analysis. *Computers & structures*, 40(4):1027–1031, 1991.

[7] JD Whitcomb and K Woo. Application of iterative global/local finite-element analysis. part 1: Linear analysis. *Communications in numerical methods in engineering*, 9(9):745–756, 1993.

[8] T Yamaguchi and H Okuda. Zooming method for FEA using a neural network. *Computers and Structures*, 247:106480, 2021.

[9] AK Noor. Global-local methodologies and their application to nonlinear analysis. *Finite Elements in Analysis and Design*, 2(4):333–346, 1986.

[10] J Whitcomb and K Woo. Global/local finite element analysis of geometrically nonlinear structures. In *33rd Structures, Structural Dynamics and Materials Conference*, page 2236, 1992.

[11] M Akterskaia, E Jansen, SR Hallett, PM Weaver, and R Rolfes. Progressive failure analysis using global-local coupling including intralaminar failure and debonding. *AIAA Journal*, pages 3078–3089, 2019.

[12] E Pietropaoli and A Riccio. A global/local finite element approach for predicting interlaminar and intralaminar damage evolution in composite stiffened panels under compressive load. *Applied Composite Materials*, 18(2):113–125, 2011.

[13] R Krueger and TK O'Brien. A shell/3d modeling technique for the analysis of delaminated composite laminates. *Composites Part A: applied science and manufacturing*, 32(1):25–44, 2001.

[14] R Krueger and PJ Minguet. Analysis of composite skin–stiffener debond specimens using a shell/3d modeling technique. *Composite Structures*, 81(1):41–59, 2007.

[15] XC Sun and SR Hallett. Barely visible impact damage in scaled composite laminates: Experiments and numerical simulations. *International Journal of Impact Engineering*, 109:178–195, 2017.

[16] A Riccio, A De Luca, G Di Felice, and F Caputo. Modelling the simulation of impact induced damage onset and evolution in composites. *Composites Part B: Engineering*, 66:340–347, 2014.

[17] F Caputo, A De Luca, G Lamanna, V Lopresto, and A Riccio. Numerical investigation of onset and evolution of lvi damages in carbon–epoxy plates. *Composites Part B: Engineering*, 68:385–391, 2015.

[18] E Carrera, M Cinefra, M Petrolo, and E Zappino. *Finite element analysis of structures through unified formulation.* John Wiley & Sons, 2014.

[19] AG de Miguel, I Kaleel, MH Nagaraj, A Pagani, M Petrolo, and E Carrera. Accurate evaluation of failure indices of composite layered structures via various fe models. *Composites Science and Technology*, 167:174–189, 2018.

[20] I Kaleel, M Petrolo, AM Waas, and E Carrera. Micromechanical progressive failure analysis of fiber-reinforced composite using refined beam models. *Journal of Applied Mechanics*, 85(2), 2018.

[21] I Kaleel, M Petrolo, E Carrera, and AM Waas. Computationally efficient concurrent multiscale framework for the nonlinear analysis of composite structures. *AIAA Journal*, 57(9):4029–4041, 2019.

[22] MH Nagaraj, I Kaleel, E Carrera, and M Petrolo. Contact analysis of laminated structures including transverse shear and stretching. *European Journal of Mechanics-A/Solids*, 80:103899, 2020.

[23] MH Nagaraj, I Kaleel, E Carrera, and M Petrolo. Nonlinear analysis of compact and thin-walled metallic structures including localized plasticity under contact conditions. *Engineering Structures*, 203:109819, 2020.

[24] MH Nagaraj, J Reiner, R Vaziri, E Carrera, and M Petrolo. Progressive damage analysis of composite structures using higher-order layer-wise elements. *Composites Part B: Engineering*, page 107921, 2020.

[25] MH Nagaraj, E Carrera, and M Petrolo. Progressive damage analysis of composite laminates subjected to low-velocity impact using 2d layer-wise structural models. *International Journal of Non-Linear Mechanics*, 127:103591, 2020.

[26] E Carrera, AG de Miguel, M Filippi, I Kaleel, A Pagani, M Petrolo, and Eo Zappino. Global-local plug-in for high-fidelity composite stress analysis in femap/nx nastran. *Mechanics of Advanced Materials and Structures*, pages 1–7, 2019.

[27] M Petrolo, MH Nagaraj, I Kaleel, and E Carrera. A global-local approach for the elastoplastic analysis of compact and thin-walled structures via refined models. *Computers & Structures*, 206:54–65, 2018.

[28] A Forghani, N Zobeiry, A Poursartip, and R Vaziri. A structural modelling framework for prediction of damage development and failure of composite laminates. *Journal of Composite Materials*, 47(20-21):2553–2573, 2013.

[29] J Reiner, T Feser, D Schueler, M Waimer, and R Vaziri. Comparison of two progressive damage models for studying the notched behavior of composite laminates under tension. *Composite Structures*, 207:385–396, 2019.

[30] AS Kaddour, MJ Hinton, PA Smith, and S Li. Mechanical properties and details of composite laminates for the test cases used in the third world-wide failure exercise. *Journal of Composite Materials*, 47(20-21):2427–2442, 2013.

[31] J Reiner, N Zobeiry, R Vaziri, T Feser, M Waimer, D Schueler, and N Toso-Pentecôte. Prediction of damage progression in notched tensile specimens: comparison between two intralaminar damage models. In *VI ECCOMAS Thematic Conference on the Mechanical Response of Composites*. Eindhoven, Netherlands, 2017.

[32] M Shahbazi. *An efficient virtual testing framework to simulate the progression of damage in notched composite laminates*. PhD thesis, University of British Columbia, 2017.

[33] C Bisagni, R Vescovini, and CG Dávila. Single-stringer compression specimen for the assessment of damage tolerance of postbuckled structures. *Journal of Aircraft*, 48(2):495–502, 2011.

[34] Z Hashin. Failure criteria for unidirectional fiber composites. *Journal of applied mechanics*, 47(2):329–334, 1980.

[35] JC Brewer and PA Lagace. Quadratic stress criterion for initiation of delamination. *Journal of composite materials*, 22(12):1141–1155, 1988.

[36] BG Green, MR Wisnom, and SR Hallett. An experimental investigation into the tensile strength scaling of notched composites. *Composites Part A: Applied Science and Manufacturing*, 38(3):867–878, 2007.

[37] N Zobeiry, R Vaziri, and A Poursartip. Characterization of strain-softening behavior and failure mechanisms of composites under tension and compression. *Composites Part A: Applied Science and Manufacturing*, 68:29–41, 2015.